New Mechanism for the α to ω Martensitic Transformation in Pure Titanium

D. R. Trinkle,[1,2] R. G. Hennig,[1] S. G. Srinivasan,[2] D. M. Hatch,[3] M. D. Jones,[4] H. T. Stokes,[3]
R. C. Albers,[2] and J. W. Wilkins[1]

[1]*The Ohio State University, Columbus, Ohio 43210, USA*
[2]*Los Alamos National Laboratory, Los Alamos, New Mexico 87545, USA*
[3]*Brigham Young University, Provo, Utah 84602, USA*
[4]*State University of New York, Buffalo, New York 14260, USA*

(Received 7 January 2003; published 11 July 2003)

We propose a new direct mechanism for the pressure driven $\alpha \rightarrow \omega$ martensitic transformation in pure titanium. A systematic algorithm enumerates all possible pathways whose energy barriers are evaluated. A new, homogeneous pathway emerges with a barrier at least 4 times lower than other pathways. The pathway is shown to be favorable in any nucleation model.

DOI: 10.1103/PhysRevLett.91.025701 PACS numbers: 64.70.Kb, 05.70.Fh, 81.30.Kf

Martensitic transformations are abundant in nature and are commonly used in engineering technologies [1]. Materials from steel to shape-memory alloys are governed by their underlying martensitic transformations [2]. The pressure driven α(hcp) $\rightarrow$ ω(hexagonal) transformation in pure titanium [3] has significant technological implications in the aerospace industry because ω phase formation lowers toughness and ductility. This transformation, first observed by Jamieson [4], has been extensively studied using static high-pressure [5] and shock-wave methods [6]. Because of experimental difficulties in directly observing martensitic transformation pathways, they are inferred from the orientation relationships between the initial and final phases. Such an approach may result in multiple transformation pathways for a given set of orientation relations, requiring one to guess the appropriate transformation pathway. Thus, despite several attempts, the pathway for this transformation is still unclear.

We calculate the energy barrier for homogeneous transformation for different titanium $\alpha \rightarrow \omega$ transformation pathways. We systematically generate and sort possible $\alpha \rightarrow \omega$ pathways by their energy barriers. A new direct pathway emerges whose barrier is lower than any other pathway, remaining favorable in any nucleation model.

Figure 1 shows our new low energy barrier pathway for the titanium $\alpha \rightarrow \omega$ transformation, called TAO-1 (''titanium alpha to omega''). This direct six-atom transformation proceeds without a metastable intermediate phase and has small shuffles and strains. The six atoms divide into a group of four atoms that shuffle by 0.63 Å and two atoms by 0.42 Å. Combining these shuffles with strains of $e_{xx} = -0.09$, $e_{yy} = 0.12$, and $e_{zz} = -0.02$ produces a final ω cell from our α cell. The original α matrix is oriented relative to the ω matrix such that $(0001)_\alpha \parallel (0\bar{1}11)_\omega$ and $[11\bar{2}0]_\alpha \parallel [01\bar{1}1]_\omega$. These orientation relations are seen in some experiments, but not in others [5,6,8].

Our pathway identification method matches (i) possible supercells of α and ω to determine the lattice strain and (ii) atom positions to determine the necessary internal relaxations, similar to [9]; details will be published elsewhere. While there are infinitely many possible supercells, we consider only 6 and 12 atom supercells with principal strains less than 0.33 and greater than -0.25. For each supercell, there is an infinite number of ways to shuffle the atom positions from α to ω; we restrict the search to the finite set of pathways where, relative to the center of mass, no atom moves more than 2.0 Å. We eliminate possible pathways that require atoms to come too close during the transformation: For a given supercell, we study the pathway with the largest closest approach distance and all pathways for that supercell with a closest approach distance within 0.1 Å of that value.

To efficiently compare the enthalpy barriers of the possible pathways, we use three methods of increasing computational sophistication and accuracy. (i) For each pathway, we calculate an approximate barrier based only on the strain, using the elastic and harmonic approximations. The ''elastic barrier'' calculation relies only on the elastic constants for each phase and the supercell geometry; it can be derived using a biquadratic approximation of the energy over the transformation range [10]. (ii) For pathways with a low elastic barrier, we calculate an energy landscape $E(\varepsilon, \delta)$ using a linear interpolation for both the cell shape and atomic positions, represented by the strain variable ε and the concerted-shuffle variable δ, respectively. The energies are calculated using a tight-binding (TB) model [11] on a grid between α at $E(0, 0)$ and ω at $E(1, 1)$. The energy at the transition state in this reduced space gives a ''landscape barrier.'' (iii) For pathways with the lowest landscape barriers, we calculate the exact barrier using the nudged elastic band (NEB) method [12] together with our TB model [11] or *ab initio* VASP (Vienna *ab initio* simulation package) simulations [13], or both. During the NEB calculation, the cell shape and size are allowed to change in response to the applied pressure. In addition, all of the atomic degrees of freedom are allowed to relax in the pathway, thus determining the exact energy barrier. The TB-NEB barrier is bounded

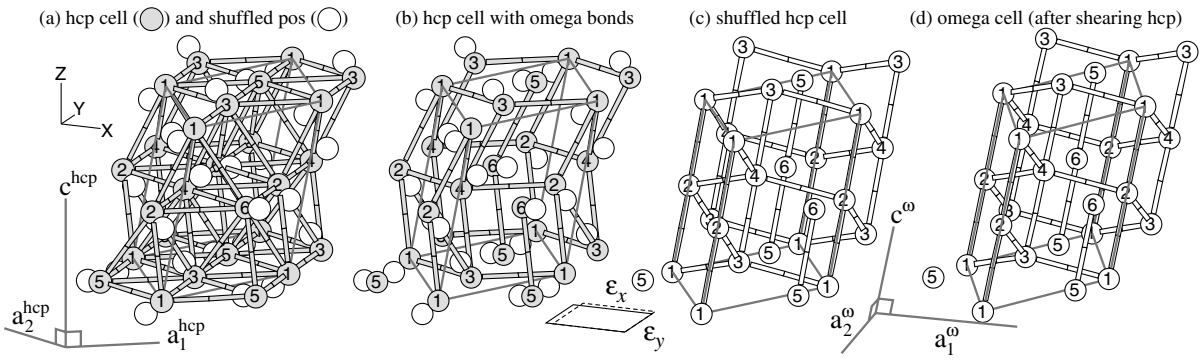

FIG. 1. Our proposed $\alpha \rightarrow \omega$ transformation pathway (TAO-1). The direct six-atom transformation is visualized (i) as a two-step process and (ii) with 21 additional atoms outside the heavy gray parallelepiped supercell. In α, atoms 1, 3, 5 and 2, 4, 6 are in the A and B stacking planes, respectively; whereas in ω, atoms 1–4 are in the Wyckoff d position of space group $P6/mmm$, and atoms 5–6 are in the Wyckoff a position [7]. (a) The gray atoms in the α cell shuffle to new positions (white atoms), with atoms 1–4 shuffling 0.63 Å, and atoms 5–6 shuffling 0.42 Å. (b) The α cell is redrawn with the "bonds" of the ω structure. Step 1: shuffling the gray atoms to the white positions, the α cell (b) produces a strained ω cell (c), contained in the same supercell. Step 2: straining the supercell (c) $e_{xx} = -0.09$, $e_{yy} = 0.12$, and $e_{zz} = -0.02$ produces the final ω supercell (d). The orientation relations connecting the α and ω supercells are $(0001)_\alpha \parallel (0\bar{1}11)_\omega$ and $[11\bar{2}0]_\alpha \parallel [01\bar{1}1]_\omega$.

above by the TB landscape barrier — due to the neglect of relaxations — and below by the elastic barrier — due to the missing shuffle contribution. The most probable pathway should have the smallest *ab initio* NEB barrier.

We calculate total energies using a TB model and carefully converged *ab initio* calculations. The TB calculations are performed using the molecular dynamics code OHMMS (object-oriented high-performance multiscale material simulator) [14] and use Mehl and Papaconstantopoulos's functional form [11] with parameters refit to reproduce full-potential density-functional total energies for hcp, bcc, fcc, omega, and simple cubic to within 0.5 meV/atom. For each pathway, we use a k-point mesh equivalent to $12 \times 12 \times 8$ in hcp with a 63 meV thermal smearing to give an energy convergence of 1 meV/atom. For our *ab initio* calculations [15] we include $3p$ electrons in the valence band and use a plane-wave kinetic-energy cutoff of 400 eV and a $7 \times 7 \times 7$ k-point mesh to ensure energy convergence to within 1 meV/atom. We relax the atomic positions and the unit cell shape and volume until the total electronic energy changes by less than 1 meV and the atomic forces are less than 20 meV/Å.

The elastic and landscape energy barrier calculations reduce our initial set of 977 candidate pathways to the three lowest barrier pathways. From the initial list of 134 supercells, we reject all but 57 because their elastic barriers are large (greater than 100 meV/atom). For the remaining 57 supercells, we generate 977 pathways (6 6-atom pathways and 971 12-atom pathways) and compute TB landscape barriers. Figure 2 shows that the elastic barrier underestimates the landscape barrier. Here we study the three pathways with the smallest landscape barriers: TAO-1, TAO-2, and Silcock [10].

Figure 3 illustrates the Silcock pathway [19]. Her pathway, deduced from observed orientation relations, involves significant atomic shuffle, relatively small strains, and is a direct transformation pathway with no intermediate state. In each α stacking plane, three of six atoms shuffle by 0.74 Å along $[11\bar{2}0]_\alpha$, while the other three shuffle in the opposite direction $[\bar{1}\bar{1}20]_\alpha$. This shuffle is accompanied by a strain $e_{xx} = 0.05$ along $[1\bar{1}00]_\alpha$ and $e_{yy} = -0.05$ along $[11\bar{2}0]_\alpha$ to produce a

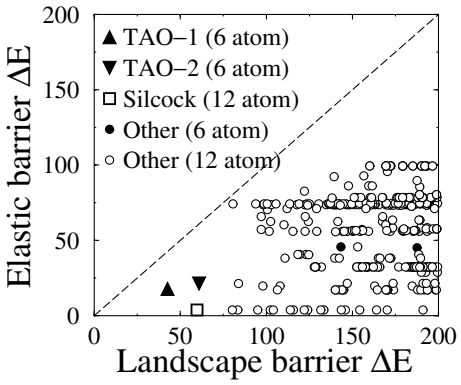

FIG. 2. Approximate elastic energy barrier (meV/atom) versus landscape energy barrier (meV/atom) for 359 pathways whose landscape barrier is below 200 meV/atom. Of the 134 supercells generated, 57 had low (less than 100 meV/atom) elastic barriers. From those 57 supercells, 977 pathways were generated; for those 977 pathways, we calculate a shear/shuffle energy landscape using our tight-binding parameters. Of those 977, 359 pathways had an elastic barrier below 200 meV/atom. We select the three pathways in the bottom left corner — TAO-1, TAO-2, and Silcock — and calculate their true barrier using the *ab initio* NEB method.

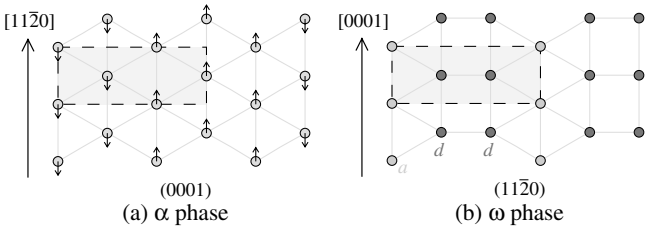

FIG. 3. Silcock pathway for α to ω transformation (single α stacking plane shown). (a) In each stacking plane, three out of every six atoms shuffle by 0.74 Å along $[11\bar{2}0]_\alpha$, while the other three shuffle in the opposite direction $[\bar{1}\bar{1}20]_\alpha$. (b) This creates the $(11\bar{2}0)_\omega$ plane from $(0001)_\alpha$. The a and d Wyckoff positions of $P6/mmm$ are also shown. This shuffle is accompanied by a strain $e_{xx} = 0.05$ along $[1\bar{1}00]_\alpha$ and $e_{yy} = -0.05$ along $[11\bar{2}0]_\alpha$ to produce a hexagonal ω cell with the correct c/a ratio. The orientation relations connecting the α and ω supercells are $(0001)_\alpha \parallel (11\bar{2}0)_\omega$ and $[11\bar{2}0]_\alpha \parallel [0001]_\omega$.

hexagonal ω cell with the correct c/a ratio. Despite the lack of direct evidence for the Silcock pathway, it is still widely invoked to describe the $\alpha \rightarrow \omega$ transformation because it is a direct pathway [20].

The remaining two pathways, TAO-1 and TAO-2, are related to Usikov and Zilbershtein's [8] proposed composite pathway involving the thermodynamically unstable β(bcc) intermediary phase, and proceeding as $\alpha \rightarrow \beta \rightarrow \omega$. Using the α-ω orientation relations, they proposed an $\alpha \rightarrow \beta$ transformation via an inverse Burgers pathway [21] followed by a $\beta \rightarrow \omega$ transformation via the collapse of two out of three $(111)_\beta$ planes. This produced two unique pathways, called variant I and variant II, depending on the direction of $\{111\}_\beta$ planes to collapse.

TABLE I. Comparison of TAO-1, TAO-2, and Silcock pathways. Energy barriers: Four different methods for calculating the energy barrier for the three pathways are shown, from least accurate to most accurate. The elastic barrier accounts only for the strain in each pathway. The landscape barrier uses a simple combined shuffle for each, and a tight-binding total energy. Finally, the NEB calculation is done with the tight-binding method and *ab initio* to accurately determine the barrier. Orientation relations: the relative orientation of α to ω is shown for each pathway. NB: Silcock and TAO-2 pathways have the same orientation relations.

	TAO-1	TAO-2	Silcock
Homogeneous barriers (in meV/atom)			
Elastic:	18	21	3.7
Landscape:	41	59	59
TB-NEB:	24	52	54
Ab initio NEB:	9	58	31
Transformation information			
Orientation relations:	$(0001)_\alpha \parallel (0\bar{1}11)_\omega$ $[11\bar{2}0]_\alpha \parallel [01\bar{1}1]_\omega$		$(0001)_\alpha (11\bar{2}0)_\omega$ $[11\bar{2}0]_\alpha \parallel [0001]_\omega$

The TAO-1 and TAO-2 pathways could have been constructed from variants I and II, respectively, by using the β intermediate system to construct a six atom supercell. Allowing variants I and II to relax *away* from the β phase would have resulted in direct transformation pathways.

Table I summarizes the energy barriers for the three pathways of interest; TAO-1 has the lowest energy barrier that best trades off between shuffle and strain. During the transformation, the closest nearest-neighbor distance is 2.63 Å, which is larger than the 2.55 Å value for TAO-2 and 2.57 Å for Silcock. Because the nearest-neighbor distances in α and ω are 2.95 Å and 2.65 Å, respectively, it is not surprising that TAO-1 has the lowest barrier. The Usikov and Zilbershtein pathway [8], passing through the intermediate β phase, has a 108 meV/atom barrier.

Figure 4 shows the enthalpy along the $\alpha \rightarrow \omega$ transformation path for the three pathways as a function of pressure. Our calculation shows ω slightly lower in energy than α at 0 GPa. The crystal structure at 0 K has not been determined experimentally; however, extrapolation of the α-ω phase boundary indicates ω as the ground state [3]. As pressure increases, the enthalpy of ω relative to α drops, and all three pathways decrease their enthalpy barrier. For the next four lowest landscape barrier pathways in Fig. 2, we find 0 GPa *ab initio* NEB barriers of 32, 37, 68, and 69 meV/atom. The barrier of the TAO-1 pathway is lowest, even up to 40 GPa.

The TAO-1 pathway remains favorable in any nucleation model because the formation energy of the critical nucleus per atom is too small to affect the energy ordering; hence, our pathway prediction will not change in the real material. Nuclei of new material grow only if they are larger than a critical size, i.e., where the nucleation energy is a maximum. In any nucleation model, the nucleus formation energy as a function of nucleus size $E(N)$ consists of an interface and a volume term: $E = \sigma N^{2/3} - \eta N$. A reasonable assumption is that the interfacial energy σ is similar (within a factor of 1.5) for all three pathways in Table I. The volume term η is given by the enthalpy difference and lattice mismatch between the phases. All three pathways possess a plane with no lattice shear during the transformation, so the nuclei can grow with only a volume mismatch. Thus, η and the critical nucleus size are the same for all three pathways. The formation energy of the critical nucleus per atom, E_c/N_c, is given by $\eta/2$, which we compare to the energy barrier per atom of our pathways. We use the enthalpy difference at the experimental shock transition pressure of 10 GPa (20 meV/atom), and the elastic stress from the volume difference (3 meV/atom), giving $\eta =$ 17 meV/atom and $E_c/N_c = 8.5$ meV/atom. The only pathway with a comparable barrier is TAO-1, and all others are a factor of 4 or more larger. Even if we consider a σ for TAO-1 that is greater by 1.5 over the other pathways, E_c and N_c would change only by a factor of 3.4, still favoring TAO-1.

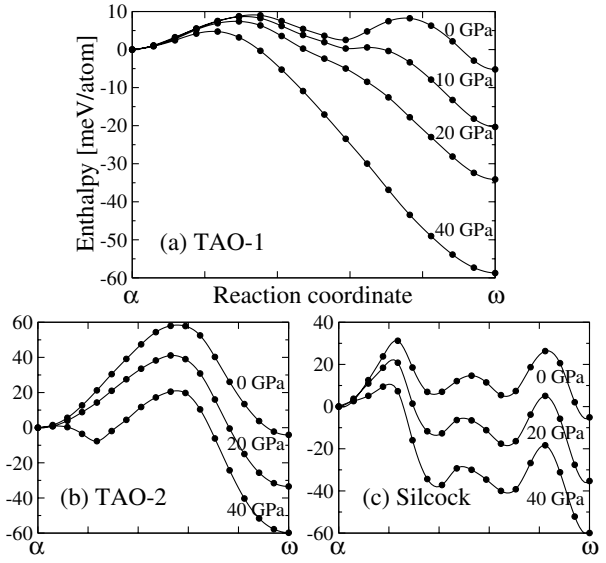

FIG. 4. Enthalpy barrier vs pressure for the three lowest energy pathways, using *ab initio* NEB with 16 intermediate states. The *ab initio* NEB gives the $T = 0$ energy along the homogeneous $\alpha \rightarrow \omega$ pathway for each pathway. The enthalpy barriers decrease with increasing pressure. (a) The TAO-1 pathway gives the smallest barrier by a factor of 4 at 0 GPa. The TAO-2 pathway (b) and Silcock pathway (c) have larger barriers at 0 GPa, an ordering which continues even at 40 GPa.

Our systematic search, involving both tight-binding and *ab initio* calculations, combined with a nucleation analysis leads to the direct TAO-1 pathway as the preferred $\alpha \rightarrow \omega$ pathway in pure titanium. By generating and comparing all relevant possible pathways, our approach finds the lowest barrier pathway for any martensitic phase transformation, providing a starting point for subsequent studies.

We thank G.T. Gray III and C.W. Greeff for helpful discussions and M.I. Baskes and R.B. Schwarz for reviewing the manuscript. D.R.T. thanks Los Alamos National Laboratory for its hospitality and acknowledges support from a Fowler Fellowship at The Ohio State University. This research is supported by DOE Grants No. DE-FG02-99ER45795 (OSU) and No. W-7405-ENG-36 (LANL). Computational resources were provided by the Ohio Supercomputing Center and NERSC.

[1] *Martensite*, edited by G. B. Olson and W. S. Owen (ASM, Metals Park, OH, 1992), p. 1.
[2] *Shape Memory Materials*, edited by K. Otsuka and C. M. Wayman (Cambridge University Press, Cambridge, 1998), p. 1.
[3] For a review article, see S. K. Sikka, Y. K. Vohra, and R. Chidambaram, Prog. Mater. Sci. **27**, 245 (1982).
[4] J. C. Jamieson, Science **140**, 72 (1963).
[5] A. Jayaraman, W. Klement, Jr., and G. C. Kennedy, Phys. Rev. **131**, 644 (1963); V. A. Zilbershtein, G. I. Nosova, and E. I. Estrin, Fiz. Met. Metalloved. **35**, 584 (1973); Y. K. Vohra, S. K. Sikka, S. N. Vaidya, and R. Chidambaram, J. Phys. Chem. Solids **38**, 1293 (1977); H. Xia *et al.*, Phys. Rev. B **42**, 6736 (1990); Y. K. Vohra and P. T. Spencer, Phys. Rev. Lett. **86**, 3068 (2001).
[6] R. G. McQueen *et al.*, in *High-Velocity Impact Phenomenon*, edited by R. Kinslow (Academic Press, New York, London, 1970), p. 293; A. R. Kutsar, V. N. German, and G. I. Nosova, Dokl. Akad. Nauk SSSR **213**, 81 (1973) [Sov. Phys. Dokl. **18**, 733 (1974)]; G. T. Gray III, C. E. Morris, and A. C. Lawson, in *Titanium 1992—Science and Technology*, edited by F. H. Froes and I. L. Caplan (TMS, Warrendale, PA, 1993), p. 225; S. V. Razorenov *et al.*, High Press. Res. **13**, 367 (1995); R. F. Trunin, G. V. Simakov, and A. B. Medvedev, High Temp. **37**, 851 (1999); C. W. Greeff, D. R. Trinkle, and R. C. Albers, J. Appl. Phys. **90**, 2221 (2001).
[7] *International Tables for Crystallography*, edited by T. Hahn (Kluwer Academic, London, 2002), Vol. A.
[8] M. P. Usikov and V. A. Zilbershtein, Phys. Status Solidi (a) **19**, 53 (1973).
[9] H. T. Stokes and D. M. Hatch, Phys. Rev. B **65**, 144114 (2002); S. G. Srinivasan *et al.*, cond-mat/0209530.
[10] See EPAPS Document No. E-PRLTAO-91-055325 for the derivation of the elastic landscape barrier and for supercell geometries, atomic coordinates, shuffles, and strains of the seven lowest energy transformation pathways. This document may be found in the online article's HTML reference section, via the EPAPS homepage (http://www.aip.org/pubservs/epaps.html), or from ftp.aip.org in the directory /epaps/. See the EPAPS homepage for more information.
[11] M. J. Mehl and D. A. Papaconstantopoulos, Phys. Rev. B **54**, 4519 (1996); Europhys. Lett. **60**, 248 (2002); D. R. Trinkle *et al.* (unpublished).
[12] H. Jónsson, G. Mills, and K.W. Jacobsen, in *Classical and Quantum Dynamics in Condensed Phase Simulations*, edited by B. J. Berne, G. Ciccotti, and D. F. Coker (World Scientific, Singapore, 1998), p. 385.
[13] G. Kresse and J. Hafner, Phys. Rev. B **47**, RC558 (1993); G. Kresse and J. Furthmüller, Phys. Rev. B **54**, 11 169 (1996).
[14] J. N. Kim, OHMMS home page, 2003, retrieved 29 April 2003 from http://www.mcc.uiuc.edu/ohmms
[15] VASP [13] is a plane-wave based code using ultrasoft Vanderbilt-type pseudopotentials [16] as supplied by Kresse and Hafner [17]. The calculations were performed using the generalized gradient approximation of Perdew and Wang [18].
[16] D. Vanderbilt, Phys. Rev. B **41**, 7892 (1990).
[17] G. Kresse and J. Hafner, J. Phys. Condens. Matter **6**, 8245 (1994).
[18] J. P. Perdew and Y. Wang, Phys. Rev. B **45**, 13 244 (1992).
[19] J. M. Silcock, Acta Metall. **6**, 481 (1958); A. Rabinkin, M. Talianker, and O. Botstein, Acta Metall. **29**, 691 (1981).
[20] A. V. Dobromyslov and N. I. Taluts, Phys. Met. Metallogr.. **69**, 98 (1990); H. Dannak, A. Dunlop, and D. Lesueur, Philos. Mag. A **79**, 147 (1999).
[21] W. G. Burgers, Physica (Utrecht) **1**, 561 (1934).